Large-order behavior of lattice strong-coupling expansions

Carl M. Bender and Lawrence R. Mead
Department of Physics, Washington University, St. Louis, Missouri 63130

L. M. Simmons, Jr.
Los Alamos National Laboratory, Los Alamos, New Mexico 87545
(Received 14 January 1983)

We examine the lattice strong-coupling expansion for the ground-state energy of the quantum-mechanical Hamiltonian $\frac{1}{2}p^2+g\,|\,x\,|^{\alpha}$, $\alpha>0$. We are interested in the large-order behavior of this series for various values of α. Treated as a quantum field theory, this simple model provides a laboratory for investigating the fascinating subtleties that arise when there are cancellations among graphs. The parameter α distinguishes between regions in which these cancellations occur with varying degrees of complexity. This paper considers various approaches to this very difficult problem and presents a partial solution.

I. INTRODUCTION

Recently there has been much research on the large-order behavior of Feynman perturbation expansions in quantum field theory.[1] The approaches used in field theory were first developed and tested by analyzing the large-order behavior of the Rayleigh-Schrödinger perturbation series for the anharmonic oscillator and other quantum-mechanical models. A general feature of all field theories for which the large-order behavior has been successfully analyzed is that the graphs in a given order *add in phase.* Superrenormalizable theories such as $(g\varphi^4)_d$, $d<4$, are examples of theories whose large-order behavior is understood. Roughly speaking, when n is large, the graphs in nth order form a sharply peaked statistical distribution in which the dominant graphs have the value g^nC^n, where C is a constant that depends on the dimension of space-time d ($C=\frac{3}{16}$ when $d=1$). Since there are approximately $n!16^n$ nth-order graphs in a $g\varphi^4$ theory when n is large, the nth term in the Feynman series has the approximate value $(16C)^n n!g^n$. Renormalizable theories such as quantum electrodynamics and $g\varphi^4$ in four dimensions have not been successfully analyzed because the graphs do not add in phase and the resulting cancellations have a drastic effect on the large-order behavior. Moreover, because of coupling-constant renormalization, individual graphs in such theories can grow much faster than C^n; specific classes of graphs[2] have been shown to grow like $n!$ This combination of very large values for graphs and complicated cancellations between them has so far proved too formidable a problem to overcome and the large-order behavior of perturbation theory for such theories is not yet understood.

In this paper we examine the lattice strong-coupling perturbation series for the ground-state energy of the quantum-mechanical Hamiltonian

$$H=\tfrac{1}{2}p^2+g\,|\,x\,|^{\alpha}\,. \tag{1.1}$$

We will see that there are cancellations among graphs contributing to the nth term in the perturbation expansion. We will also identify specific graphs that grow like a factorial of n (these graphs are large not because of renormalization effects but because the vertices of the graphs grow rapidly with n). Thus, the simple model in (1.1) exhibits all of the properties that make the large-order behavior of renormalizable quantum field theories so hard to determine. This model is interesting because it provides a laboratory for investigating the subtleties in the fact that there are complicated cancellations among large numbers of graphs.[3] The parameter α is crucial because, as we will show, it distinguishes between regions in which the cancellations occur with varying degrees of complexity.

The notation and graphical rules for the lattice strong-coupling expansion for the ground-state energy $E_0(\alpha)$ of the Hamiltonian in (1.1) have been derived elsewhere.[4] We review them very briefly. A dimensional argument shows that the ground-state energy $E_0(\alpha)$ can be expressed as a pure dimensionless number $\epsilon(\alpha)$ times an appropriate power of g:

$$E_0(\alpha)=\epsilon(\alpha)g^{2/(\alpha+2)}\,. \tag{1.2}$$

Introducing a lattice enables us to express $\epsilon(\alpha)$ as the lattice limit of a series in powers of the dimensional lattice parameter $x=\alpha^{-(2+\alpha)/\alpha}g^{-2/\alpha}$:

$$\epsilon(\alpha)=\frac{\alpha+2}{2\alpha}\lim_{x\to\infty}x^{\alpha/(\alpha+2)}\left[1+\sum_{n=1}^{\infty}x^nC_n\right]\,. \tag{1.3}$$

We refer to C_n as the nth term in the lattice strong-coupling perturbation series. In Ref. 4, the first 12 coefficients $C_1,\ldots,C_{12}$ are computed for all values of α.

To calculate C_n we use the following graphical procedure: Draw all n-line connected graphs having no external legs. These graphs must have an even number of lines emerging from every vertex. The $2n$-point vertices are assigned the value V_{2n}, where

$$\ln\left[\frac{F(J)}{F(0)}\right]=\sum_{n=1}^{\infty}\frac{J^{2n}}{(2n)!}V_{2n} \tag{1.4}$$

and

$$F(J)=\int_{-\infty}^{\infty} dx\, e^{-Jx-|x|^{\alpha}}$$
$$=F(0)\sum_{n=0}^{\infty}\frac{J^{2n}W_{2n}}{(2n)!}\ , \tag{1.5}$$
$$W_{2n}=\Gamma\left[\frac{2n+1}{\alpha}\right]\Big/\Gamma(1/\alpha)\ . \tag{1.6}$$

The first few vertex factors are

$$V_2=\Gamma(3/\alpha)/\Gamma(1/\alpha)\ ,$$
$$V_4=\Gamma(5/\alpha)/\Gamma(1/\alpha)-3\Gamma^2(3/\alpha)\Gamma^2(1/\alpha)\ ,$$
$$V_6=\Gamma(7/\alpha)\Gamma(1/\alpha)-15\Gamma(5/\alpha)\Gamma(3/\alpha)/\Gamma^2(1/\alpha)$$
$$+30\Gamma^3(3/\alpha)/\Gamma^3(1/\alpha)\ .$$

The lines are represented in coordinate space as the lattice equivalent of the inverse boson propagator $\delta''(x-y)$: a line connecting the vertices i and j has the form

$$\delta_{i,j+1}-2\delta_{ij}+\delta_{i+1,j}\ . \tag{1.7}$$

Lattice sums must be performed over all vertices but one.

To evaluate a graph we multiply together the symmetry number for the graph, the values of the vertices in the graph, and the result of performing the lattice sum. To obtain C_n we combine the results for all connected n-line graphs and multiply the result by $2n$. (The factor of $2n$ arises because, as explained in Ref. 4, it is simplest to find the lattice series for $g\,dE/dg$ and this differentiation introduces the extra factor of $2n$.)

In this paper we attempt to determine the behavior of C_n for large n for various values of α. We will show that there are three distinct regions of α to consider. When $0<\alpha<1$ the C_n grow very rapidly with n. In this region the asymptotic behavior of C_n for large n is easy to derive because we can identify the largest graphs and evaluate them in closed form. When $1\le\alpha<2$ the C_n do not grow as rapidly with n, but the series in (1.3) is still divergent for all x. This region is difficult to analyze because there is a cancellation among graphs; C_n grows less rapidly with n than the individual graphs. This cancellation prevents us from obtaining the precise asymptotic behavior of C_n. However, it appears that in this region the cancellation can be treated approximately by various methods, and we obtain good estimates for the growth of C_n. When $\alpha\ge 2$ the cancellation among graphs occurs on a very profound and subtle level. The cancellation is so strong that the series in (1.3) has a finite radius of convergence. We do not know how to treat this case analytically.

Here is a detailed summary of the results that are obtained throughout the rest of this paper.

Region 1: $0<\alpha<1$. Note that for these values of α the integral in (1.5) does not exist. However, the series coefficients W_{2n} in (1.6) and V_{2n} in (1.4) do exist, and these series make sense as asymptotic series. In this region the vertices V_{2n} grow more rapidly than $(2n)!$ and are all positive,

$$V_{2n}\sim\Gamma\left[\frac{2n+1}{\alpha}\right]\Big/\Gamma\left[\frac{1}{\alpha}\right]\quad(n\to\infty)\ . \tag{1.8}$$

Because the vertices grow so rapidly we can identify one graph in nth order that dominates all others. From this, we determine the leading behavior of C_n for large n:

$$C_n\sim\frac{(-1)^n 2\Gamma((2n+1)/\alpha)}{\Gamma(n)\Gamma(1/\alpha)}\quad(n\to\infty)\ . \tag{1.9}$$

By including more graphs we obtain the higher-order corrections to the growth of C_n:

$$C_n\sim\frac{(-1)^n 2\Gamma((2n+1)/\alpha)}{\Gamma(n)\Gamma(1/\alpha)}\left[1+\frac{\Gamma((2n-1)/\alpha)\Gamma(3/\alpha)n(n-2)}{\Gamma((2n+1)/\alpha)\Gamma(1/\alpha)}+\cdots\right]\ . \tag{1.10}$$

Note that from (1.9) the Carleman condition[5] is satisfied [C_n grows no faster than $(2n)!$] when $\alpha\ge 2/3$. Thus, the series in (1.3) is Borel summable and, as shown in Ref. 4, Padé summation of (1.3) gives an accurate approximation the $\epsilon(\alpha)$. Region 1 is treated in Sec. II.

Special Case: $\alpha=1$. The value of α marks the dividing line between Regions 1 and 2. For this value of α we have an exact formula for the vertices:

$$V_{2n}=(2n)!/n\ . \tag{1.11}$$

Because the vertices no longer grow faster than $(2n)!$ when $\alpha\ge 1$, it is no longer true that a small number of graphs dominate the large-order behavior of perturbation theory.

Region 2: $1\le\alpha<2$. When $\alpha\ge 1$ the vertices V_{2n} grow in magnitude roughly like $(2n)!$ (by comparison, the vertices in Region 1 have a factorial growth that depends on α). This growth of the vertices V_{2n} for large n is established in Sec. III.

The sign pattern of V_{2n} is irregular when $2>\alpha>1$. This irregular sign pattern leads to cancellations between positive and negative graphs. This cancellation gives a lattice series whose coefficients C_n grow less rapidly than the vertices:

$$C_n\sim\frac{\Gamma((2n+1)/\alpha)}{\Gamma(n)}K^n\quad(n\to\infty)\ , \tag{1.12}$$

where K is a constant.

We present three different arguments to obtain the result in (1.12): a partial summation of graphs in Sec. IV, a graph averaging argument in Sec. V, and a lattice instanton calculation in Sec. VI. None of these arguments is sufficient to obtain the value of K.

Special Case: $\alpha=2$. This value of α separates Regions 2 and 3. For this special value of α (the harmonic oscillator) all of the vertices vanish except V_2. As a result the perturbation coefficients can be computed in closed form:

$$C_n=\frac{(-1)^n(2n)!}{2^n(n!)^2}\ . \tag{1.13}$$

Note that the lattice series has a finite radius of conver-

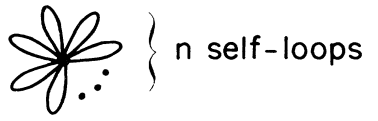

FIG. 1. The largest graph in order n when $0<\alpha<1$.

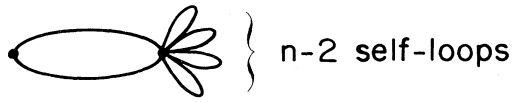

FIG. 2. The second-largest graph in order n when $0<\alpha<1$.

gence. This feature of the lattice series persists into Region 3.

Region 3: $\alpha>2$. As in Region 2, the vertices in Region 3 continue to grow like $(2n)!$. However, unlike the vertices in Region 2, the V_{2n} in Region 3 alternate in sign. This sign alternation seems to result in a much deeper cancellation among the graphs contributing to C_n. The result is that the lattice series in (1.3) has a finite radius of convergence. However, unlike the lattice series coefficients in Region 2, the C_n in Region 3 have an irregular sign pattern. As we observed in Ref. 4, the onset of the irregular sign pattern occurs earlier as α increases beyond 2. We do not know how to calculate the radius of convergence of the lattice series in Region 3. We discuss Region 3 in Sec. VII.

We include two appendices on graph counting. In Appendix A we study the asymptotic growth of the number of lattice strong-coupling graphs as n, the number of lines per graph, becomes large. In Appendix B we divide the set of all n-line graphs into distinct topological classes labeled by the number of vertices and identify the class that dominates the asymptotic estimate in Appendix A.

II. REGION 1: $0<\alpha<1$

In this region the integral in (1.5) does not exist. However, the series in (1.5) does exist as an asymptotic series. Moreover, the series in (1.4) which defines the vertices V_{2n} does exist. Since W_{2n} grows faster than $(2n)!$ as $n\to\infty$ it is easy to argue that $V_{2n}\sim W_{2n}$ as $n\to\infty$: expanding the logarithm in (1.4) and matching powers of J^{2n} gives an explicit series representation for V_{2n}:

$$\frac{V_{2n}}{(2n)!}=\frac{W_{2n}}{(2n)!}-\tfrac{1}{2}\sum_{k=1}^{n-1}\frac{W_{2k}W_{2n-2k}}{(2k)!(2n-2k)!}+\tfrac{1}{3}\sum\sum\sum+\cdots . \tag{2.1}$$

But

$$W_{2n}=\Gamma\left[\frac{2n+1}{\alpha}\right]\Big/\Gamma(1/\alpha) . \tag{2.2}$$

Thus, successive terms in (2.1) become increasingly negligible because the largest contributions come from the end points of the sums. Hence, to leading order, the vertices are all positive and

$$V_{2n}\sim\Gamma\left[\frac{2n+1}{\alpha}\right]\Big/\Gamma(1/\alpha)\quad(n\to\infty) . \tag{2.3}$$

Including the first correction term in (2.1) gives a higher-order approximation to V_{2n}:

$$V_{2n}\sim\frac{\Gamma((2n+1)/\alpha)}{\Gamma(1/\alpha)}\left[1-\frac{\Gamma((2n-1)/\alpha)\Gamma(3/\alpha)n(2n-1)}{\Gamma((2n+1)/\alpha)\Gamma(1/\alpha)}\right]\quad(n\to\infty) . \tag{2.4}$$

Because the vertices grow so rapidly with n in this region we can identify one graph in nth order which dominates over all other graphs. This graph, shown in Fig. 1, has an extremely small symmetry number, $2^{-n}/n!$, and its lattice sum is $(-2)^n$. However, the vertex V_{2n} in (2.3) grows so rapidly with n that the dominant effect in the region that determines the relative contributions of graphs is the vertex content.

Multiplying together the symmetry number, vertex factor, lattice sum, and extra factor of $2n$ according to the rules stated in Sec. I, gives the contribution of this graph to the perturbation coefficient C_n:

$$C_n\sim\frac{2(-1)^n\Gamma((2n+1)/\alpha)}{\Gamma(n)\Gamma(1/\alpha)}\quad(n\to\infty) . \tag{2.5}$$

The second-largest n-line graph is shown in Fig. 2. This graph is second largest because it contains the second-largest vertex V_{2n-2}. Note that the symmetry number for this graph is $2^{-n}/(n-2)!$. This is *larger* than the symmetry number for the graph in Fig. 1 by a factor of n^2. However, for large n, the vertex V_{2n} is larger than the vertex V_{2n-2} by a factor of $n^{2/\alpha}$. Thus, in the region where $\alpha<1$ the graph in Fig. 1 clearly dominates. When $\alpha\geq 1$ the graph in Fig. 1 ceases to be the largest graph.

We can include the contribution of the graph in Fig. 2, but we must be consistent and also include the higher-order corrections to the vertex V_{2n} in (2.4) for the graph in Fig. 1. We obtain the following higher-order correction to C_n:

$$C_n\sim\frac{2(-1)^n\Gamma((2n+1)/\alpha)}{\Gamma(n)\Gamma(1/\alpha)}\left[1+\frac{\Gamma((2n-1)/\alpha)\Gamma(3/\alpha)n(n-2)}{\Gamma((2n+1)/\alpha)\Gamma(1/\alpha)}+\cdots\right]\quad(n\to\infty) . \tag{2.6}$$

TABLE I. A comparison between the exact value of C_n, the leading-order approximation to C_n given in (2.5), and the higher-order approximation to C_n in (2.6) for $a=\frac{1}{8}$. The portion of the approximation that agrees with the exact value of C_n is underlined. The exact results are taken from Ref. 4.

n	C_n (exact)	C_n [leading-order approximation in (2.5)]	C_n [higher-order approximation in (2.6)]
3	$-2.519\,127\,711\,835\,5\times10^{69}$	$-\underline{2.519\,1276}\times10^{69}$	$-\underline{2.519\,127\,711}81\times10^{69}$
4	$5.624\,858\,393\,450\,292\times10^{97}$	$\underline{5.624\,858\,390}\times10^{97}$	$\underline{5.624\,858\,393\,44}\times10^{97}$
5	$-3.485\,048\,443\,196\,043\times10^{127}$	$-\underline{3.485\,048\,443}09\times10^{127}$	$-\underline{3.485\,048\,443\,196}038\times10^{127}$
6	$3.274\,768\,755\,460\,36\times10^{158}$	$\underline{3.274\,768\,7554}5\times10^{158}$	(exact to 16 places)
7	$-3.072\,412\,787\,262\,667\times10^{190}$	$-\underline{3.072\,412\,787\,2617}\times10^{190}$	(exact to 16 places)
8	$2.118\,349\,007\,399\,682\times10^{223}$	$\underline{2.118\,349\,007\,3995}7\times10^{223}$	(exact to 16 places)
9	$-8.490\,813\,348\,601\,395\times10^{256}$	$\underline{8.490\,813\,348\,601\,31}\times10^{256}$	(exact to 16 places)
10	$1.644\,271\,440\,102\,857\times10^{291}$	$\underline{1.644\,271\,440\,102\,853}\times10^{291}$	(exact to 16 places)
11	$-1.324\,368\,686\,557\,919\times10^{326}$	(exact to 16 places)$\times10^{326}$	(exact to 16 places)
12	$3.920\,147\,296\,082\,154\times10^{361}$	(exact to 16 places)$\times10^{361}$	(exact to 16 places)

In Tables I–V we compare the exact value of C_{2n} for $\alpha=\frac{1}{8}, \frac{1}{4}, \frac{1}{2}, \frac{2}{3}$, and 1 with the approximations given in (2.5) and (2.6). These approximations work best when α is near zero. Note that the correction term in (2.6) increases the magnitude of the leading-order approximation to C_n. This is expected because our numerical results in Tables I–V show that the leading-order approximation to C_n in (2.5) is smaller than the exact value.

III. LARGE-n BEHAVIOR OF THE VERTICES V_{2n} FOR $\alpha\geq1$

When $\alpha=1$ we have an exact formula for the vertices V_{2n} in (1.11):

$$V_{2n}=(2n)!/n\ . \tag{3.1}$$

When $\alpha>1$ we do not have such a closed-form expression for V_{2n} (except for $\alpha=2$). However, it is easy to show that for large n, V_{2n} continues to grow roughly like $(2n)!$. To do so we apply the Hadamard factorization theorem.[6]

When $\alpha>1$ the series in (1.5) converges for all J and demonstrates that $F(J)$ is an entire function. The coefficients a_n of a Taylor series define the *order* ρ of that series:

$$\frac{1}{\rho}\equiv\lim_{n\to\infty}\inf\frac{\ln(1/|a_n|)}{n\ln n}\ . \tag{3.2}$$

For the series in (1.5),

$$a_n=\frac{W_{2n}}{(2n)!}=\frac{\Gamma((2n+1)/\alpha)}{(2n)!\Gamma(1/\alpha)}\ .$$

Thus,

$$\rho=\frac{\alpha}{\alpha-1}\ . \tag{3.3}$$

The Hadamard theorem states that if $\rho>1$, $F(J)/F(0)$ has the form $e^{P(J)}F_1(J)$ where $P(J)$ is a polynomial of degree $\leq\rho$ and $F_1(J)$ is an entire function. When $F_1(J)$ is not constant it has zeros in the complex J plane.

For $1<\alpha<\infty$, we have $\rho>1$. Thus, we know that $F_1(J)$ has zeros in the complex J plane except when $\alpha=2$. [Only the special case $\alpha=2$ gives a constant for $F_1(J)$.] Thus, $\ln[F(J)/F(0)]$ has branch points in the complex J plane when $\alpha>1$ ($\alpha\neq2$). The distance R from the origin to the nearest branch point in the complex J plane is the radius of convergence of the series in (1.4). This shows that for $\alpha>1$ and $\alpha\neq2$,

TABLE II. Same as in Table I except that $\alpha=\frac{1}{4}$.

n	C_n (exact)	C_n [leading-order approximation in (2.5)]	C_n [higher-order approximation in (2.6)]
3	$-1.815\,215\,037\,526\,724\times10^{27}$	$-\underline{1.814\,811\,6}\times10^{27}$	$-\underline{1.815\,216}\,215\,332\times10^{27}$
4	$5.740\,973\,297\,123\,301\times10^{38}$	$\underline{5.740\,637\,8}\times10^{38}$	$\underline{5.740\,959}\,721\,195\times10^{38}$
5	$-8.391\,153\,809\,536\,072\times10^{50}$	$-\underline{8.391\,008\,8}\times10^{50}$	$-\underline{8.391\,151}\,976\,233\times10^{50}$
6	$4.308\,690\,083\,413\,996\times10^{63}$	$\underline{4.308\,663\,2}\times10^{63}$	$\underline{4.308\,689}\,998\,954\times10^{63}$
7	$-6.420\,531\,486\,735\,540\times10^{76}$	$-\underline{6.420\,514\,8}\times10^{76}$	$-\underline{6.420\,531}\,468\,546\times10^{76}$
8	$2.412\,113\,440\,391\,647\times10^{90}$	$\underline{2.412\,110\,5}\times10^{90}$	$\underline{2.412\,113}\,439\,450\times10^{90}$
9	$-2.051\,021\,502\,929\,257\times10^{104}$	$-\underline{2.051\,020\,2}\times10^{104}$	$-\underline{2.051\,021\,502}\,761\times10^{104}$
10	$3.624\,269\,997\,615\,144\times10^{118}$	$\underline{3.624\,268\,8}\times10^{118}$	$\underline{3.624\,269\,997}\,541\times10^{118}$
11	$-1.241\,918\,161\,696\,587\times10^{133}$	$-\underline{1.241\,917\,9}\times10^{133}$	$-\underline{1.241\,918\,161}\,689\times10^{133}$
12	$7.793\,395\,783\,031\,931\times10^{147}$	$\underline{7.793\,394\,9}\times10^{147}$	$\underline{7.793\,395\,783\,0}17\times10^{147}$

TABLE III. Same as in Table I except that $\alpha=\frac{1}{2}$.

n	C_n (exact)	C_n [leading-order approximation in (2.5)]	C_n [higher-order approximation in (2.6)]
3	$-6.350\,74\times10^{9}$	-6.227×10^{9}	-6.3577×10^{9}
4	$1.209\,22\times10^{14}$	1.186×10^{14}	1.2056×10^{14}
5	$-4.321\,36\times10^{18}$	-4.258×10^{18}	-4.3109×10^{18}
6	$2.613\,18\times10^{23}$	2.585×10^{23}	2.6097×10^{23}
7	$-2.475\,80\times10^{28}$	-2.456×10^{28}	-2.4741×10^{28}
8	$3.467\,17\times10^{33}$	3.446×10^{33}	3.4660×10^{33}
9	$-6.861\,14\times10^{38}$	-6.827×10^{38}	-6.8598×10^{38}
10	$1.851\,22\times10^{44}$	1.844×10^{44}	1.8510×10^{44}
11	$-6.615\,31\times10^{49}$	-6.593×10^{49}	-6.6148×10^{49}
12	$3.056\,52\times10^{55}$	3.048×10^{55}	3.0564×10^{55}

$$|V_{2n}|\sim(2n)!R^{-n}\quad(n\to\infty)\,. \tag{3.4}$$

[For the special case $\alpha=2$ where F_1 is a constant the series in (1.4) terminates.] Note that when $\alpha\geq1$ the controlling factor $(2n)!$ of the behavior of V_{2n} for large n is independent of α. This contrasts with the result for the behavior of V_{2n} in Region 1 ($\alpha<1$) in (2.3). Numerical computations indicate that the range $\alpha\geq1$ divides into four interesting subregions: (i) When $\alpha=1$ the V_{2n} are all positive [see (3.1)]. (ii) When $1<\alpha<2$ the V_{2n} seem to have an irregular sign pattern; the first few V_{2n} are positive, but as α increases the irregular sign pattern sets in at smaller values of n. (iii) When $\alpha=2$, $V_{2n}=0$ for $n>1$. (iv) V_{2n} alternate in sign like $(-1)^{n+1}$ when $\alpha>2$. These results are illustrated in Table VI.

IV. REGION 2: $1\leq\alpha<2$. SUMMATION OF DOMINANT GRAPHS

In Sec. II we showed that the graph in Fig. 1 contributes more to C_n than any other n-line graph and that the graph in Fig. 2 gives the second-largest contribution. These conclusions depend on the following observations: The symmetry number for the graph in Fig. 2 is larger than that for the graph in Fig. 1 by a factor of n^2, but the vertex V_{2n} is larger than V_{2n-2} by the factor $n^{2/\alpha}$, which is larger than n^2 as long as $\alpha<1$.

This simple dominance argument fails when $\alpha\geq1$ because from (3.4) we have approximately

$$\frac{V_{2n}}{V_{2n-2}}\sim n^2\quad(n\to\infty)\,. \tag{4.1}$$

Thus, the graphs in Figs. 1 and 2 are of comparable size as $n\to\infty$.

We will argue in this section that in addition to the graphs of Figs. 1 and 2 there is a large class of n-line graphs all of comparable size as $n\to\infty$. These are the largest graphs having n lines. We will show how to sum this class of graphs to obtain an estimate of C_n.

To characterize the class of largest graphs we systematically examine all n-line graphs whose largest vertex is V_{2n-2k} (we term this the *subclass* k), for k ranging from 0 to n. For each value of k it is easy to identify the largest graphs in this subclass. The graphs for $k=0$ and 1 are shown in Figs. 1 and 2.

There are four connected graphs to consider when $k=2$ and these are shown in Fig. 3. One can evaluate these graphs according to the rules given in Sec. I. The symmetry numbers for the graphs in Figs. 3(c) and 3(d) are smaller than the symmetry numbers for the graphs in Figs. 3(a) and 3(b) by a factor n. As a result, the dominant contribution to C_n from connected graphs containing V_{2n-4}, $n\to\infty$, is given by

$$\text{graph 3(a)}=(-1)^n\frac{V_{2n-4}}{(n-4)!}\frac{V_2^2I_2^2}{8} \tag{4.2}$$

and

TABLE IV. Same as in Table I except that $\alpha=\frac{2}{3}$.

n	C_n (exact)	C_n [leading-order approximation in (2.5)]	C_n [higher-order approximation in (2.6)]
3	$-1.352\,86\times10^{6}$	-1.28×10^{6}	-1.362×10^{6}
4	$6.981\,14\times10^{8}$	6.43×10^{8}	6.881×10^{8}
5	$-5.308\,41\times10^{11}$	-4.88×10^{11}	-5.197×10^{11}
6	$5.630\,48\times10^{14}$	5.21×10^{14}	5.521×10^{14}
7	$-7.990\,01\times10^{17}$	-7.47×10^{17}	-7.868×10^{17}
8	$1.466\,08\times10^{21}$	1.38×10^{21}	1.449×10^{21}
9	$-3.381\,85\times10^{24}$	-3.21×10^{24}	-3.353×10^{24}
10	$9.582\,26\times10^{27}$	9.15×10^{27}	9.522×10^{27}
11	$-3.271\,78\times10^{31}$	-3.14×10^{31}	-3.256×10^{31}
12	$1.324\,86\times10^{35}$	1.27×10^{35}	1.320×10^{35}

TABLE V. Same as in Table I except that $\alpha=1$. Here we expect that the approximations in (2.5) and (2.6) fail because the graphs we have neglected are not small when α lies outside region 1.

n	C_n (exact)	C_n [leading-order approximation in (2.5)]	C_n [higher-order approximation in (2.6)]
3	-832	-720	-864
4	1.7968×10^{4}	1.34×10^{4}	1.728×10^{4}
5	-4.5590×10^{5}	-3.02×10^{5}	-4.032×10^{5}
6	1.3190×10^{7}	7.98×10^{6}	1.089×10^{7}
7	-4.2745×10^{8}	-2.42×10^{8}	-3.353×10^{8}
8	1.5338×10^{10}	8.30×10^{9}	1.162×10^{10}
9	-6.0428×10^{11}	-3.18×10^{11}	-4.483×10^{11}
10	2.5970×10^{13}	1.34×10^{13}	1.905×10^{13}
11	-1.2108×10^{15}	-6.19×10^{14}	-8.850×10^{14}
12	6.0960×10^{16}	3.11×10^{16}	4.460×10^{16}

$$\text{graph } 3(b)=(-1)\frac{V_{2n-4}}{(n-4)!}\frac{I_4V_4}{24}\ . \tag{4.3}$$

Here I_{2l} is the result of evaluating the lattice sum for the graph consisting of two points joined by $2l$ lines (see Fig. 4):

$$I_{2l}=2+2^{2l}\ . \tag{4.4}$$

The values of the graphs in Figs. 1 and 2 are

$$\text{graph } 1=(-1)^n\frac{V_{2n}}{(n)!}\ , \tag{4.5}$$

$$\text{graph } 2=(-1)^n\frac{V_{2n-2}}{(n-2)!}\frac{I_2V_2}{2}\ . \tag{4.6}$$

Note that $V_{2n}\sim(2n)!$ so the expressions in (4.2), (4.3), (4.5), and (4.6) are all of the same order as $n\to\infty$.

It should now be evident that the largest graphs in the subclass k are those with the smallest number of self-loops, because these graphs have the largest symmetry numbers. Such graphs have no substructures other than self-loops and graphs of the form shown in Fig. 4. Thus, the three dominant graphs in the subclass $k=3$ are those shown in Fig. 5 and together they contribute

$$(-1)^n\frac{V_{2n-6}}{(n-6)!}\left[\frac{I_6V_6}{6!}+\frac{I_2V_2I_4V_4}{2!4!}+\frac{I_2{}^3V_2{}^3}{3!8}\right]\ . \tag{4.7}$$

In Fig. 6 we show some graphs in subclass $k=3$ whose contribution to C_n is negligible compared to (4.7) as $n\to\infty$. The expression (4.7) is larger than the contributions of Figs. 6(a) and 6(b) by a factor n and is larger than the contribution of Fig. 6(c) by a factor n^2, as $n\to\infty$.

Having characterized by the examples above the largest graphs of subclass k we can write a general formula for the sum S_k of the dominant graphs in subclass k:

$$S_k=(-1)^n\frac{V_{2n-2k}}{(n-2k)!}[\text{coefficient of } z^{2k} \text{ in } f(z)]\ , \tag{4.8}$$

where

$$f(z)=\exp\left[\sum_{l=1}^{\infty}\frac{V_{2l}I_{2l}z^{2l}}{(2l)!}\right]\ . \tag{4.9}$$

The sum in (4.9) can be evaluated exactly using the generating function for the vertices in (1.4). Using the expression for I_{2l} in (4.4) we obtain

$$f(z)=\exp\left[2\sum_{l=1}^{\infty}\frac{V_{2l}z^{2l}}{(2l)!}\right]\exp\left[\sum_{l=1}^{\infty}\frac{V_{2l}(2z)^{2l}}{(2l)!}\right]$$
$$=\left[\frac{F(z)}{F(0)}\right]^2\left[\frac{F(2z)}{F(0)}\right]\ . \tag{4.10}$$

Using the generating function for F in (1.5) and the definition (1.6) we can extract the coefficient of z^{2k} from (4.10) as a double sum:

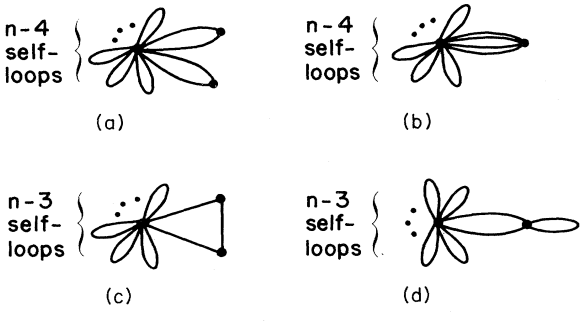

FIG. 3. All connected n-line graphs containing the vertex V_{2n-4}. As $n\to\infty$ the graphs (a) and (b) dominate the graphs (c) and (d) by a factor of order n.

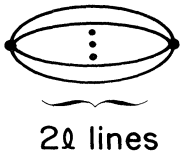

FIG. 4. The evaluation of the lattice sum for this graph gives $I_{2l}=(2+2^{2l})/(2l)!$.

$$[\text{coefficient of } z^{2k} \text{ in } f(z)] = \sum_{j=0}^{k} \sum_{l=0}^{j} \frac{\Gamma((2k-2j+1)/\alpha)\Gamma((2l+1)/\alpha)\Gamma((2j-2l+1)/\alpha)2^{2k-2j}}{(2k-2j)!(2l)!(2j-2l)![\Gamma(1/\alpha)]^3} . \tag{4.11}$$

Finally, we apply the results given above to calculate, according to the rules explained in Sec. I, the contribution of these dominant graphs to C_n. The result is

$$C_n \approx \frac{(-1)^n 2n}{[\Gamma(1/\alpha)]^3} \sum_{k=0}^{[n/2]} \frac{V_{2n-2k}}{(n-2k)!} 2^{2k} \sum_{j=0}^{k} \sum_{l=0}^{j} 2^{-2j} \frac{\Gamma((2k-2j+1)/\alpha)\Gamma((2l+1)/\alpha)\Gamma((2j-2l+1)/\alpha)}{(2k-2j)!(2l)!(2j-2l)!} . \tag{4.12}$$

This is the final expression resulting from the approximation of retaining only the largest n-line graphs of each subclass k.

In Sec. V we compare the exact values of C_n with a numerical evaluation of (4.12) and to other approximations. We will see that the approximation in (4.12) is not particularly good and the reason is important.

As illustrated in Table VI, the V_{2n} have an irregular sign pattern in the region $\alpha > 1$, and therefore cancellations among the graphs occur. In deriving (4.12) we used the exact expression for the generating function (1.4) for the vertices, thus taking into account the exact cancellations among *these* graphs. These cancellations reduce the magnitude of C_n from approximately $n!$, the value of each individual graph, to approximately $\Gamma(2n/\alpha)/n!$, as demonstrated by the exact numerical studies in Sec. V. Thus, some of the graphs that we neglected are larger than the final result in (4.12). Of course, these graphs also cancel against each other. But, it is clear that this cancellation phenomenon is not easy to treat properly and makes it extremely difficult to estimate *a priori* the accuracy of the approximation method.

V. REGION 3: $1 \leq \alpha < 2$. GRAPH-AVERAGING ARGUMENT

In this section we make the approximation that the cancellation among graphs is not very sensitive to the specific rules for calculating lattice sums. Thus, we replace the lattice sum for each n-line graph by an average lattice sum. Then we calculate C_n by summing exactly over all n-line graphs weighted by their symmetry numbers and vertices. Based on previous experience with graphical theories[7] we expect that the average lattice sum for an n-line graph behaves for large n like G^n, where G is a constant. We will see that this expectation is consistent with our numerical results and we will determine the constant G empirically and use it to estimate C_n for large n. The numerical results of this procedure are quite good.

To perform this calculation we construct a model field theory in which every n-line graph has the value G^n apart from its symmetry number and vertex content. To construct the vacuum-vacuum function Z for such a theory we combine the operator

$$\exp\left[\frac{G}{2}\frac{d^2}{dx^2}\right], \tag{5.1}$$

which inserts lines, each line weighted by G, and

$$\exp\left[\sum_{n=1}^{\infty} V_{2n}\frac{x^{2n}}{(2n)!}\right], \tag{5.2}$$

which represents the set of vertices for this theory as introduced in Sec. I. The sum of all connected vacuum graphs is given by

$$\ln Z = \ln\left[\exp\left[\frac{G}{2}\frac{d^2}{dx^2}\right]\exp\left[\sum_{n=1}^{\infty} V_{2n}\frac{x^{2n}}{(2n)!}\right]\right]_{x=0} . \tag{5.3}$$

The term containing G^n in the Taylor expansion of (5.3) is the sum of the connected vacuum graphs with n lines.

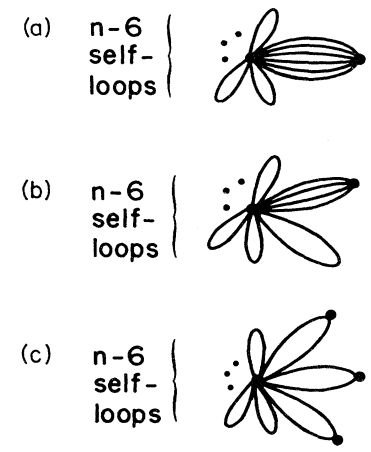

FIG. 5. The largest n-line graphs containing the vertex V_{2n-6} (subclass $k=3$).

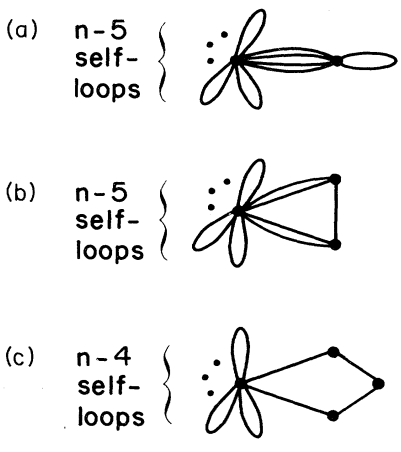

FIG. 6. Some graphs in subclass $k=3$ (n-line graphs containing the vertex V_{2n-6}) whose contribution to C_n is negligible as $n \to \infty$ compared to (4.7).

TABLE VI. The vertices V_{2n} for $n=1,2,\ldots,12$ for various values of α. Observe that in the range $1<\alpha<2$ the vertices have an irregular sign pattern but that when $\alpha>2$ the vertices alternate in sign.

n \ α	1.1	1.16	1.2	1.3	1.5	1.8	1.9	1.98	2.02	3	7
1	1.49	1.28	1.18	0.976	0.738	0.564	0.529	0.505	0.495	0.373	0.316
2	5.04	3.20	2.42	1.27	0.416	7.39×10^{-2}	3.00×10^{-2}	5.18×10^{-3}	-4.83×10^{-3}	-8.10×10^{-2}	−0.104
3	51.0	22.1	13.0	3.64	0.220	-4.99×10^{-2}	-2.59×10^{-2}	-5.05×10^{-3}	4.94×10^{-3}	0.118	0.174
4	1.00×10^{3}	2.76×10^{2}	1.19×10^{2}	12.9	−0.793	3.27×10^{-2}	3.90×10^{-2}	9.69×10^{-3}	-1.03×10^{-2}	−0.384	−0.644
5	3.15×10^{4}	5.12×10^{3}	1.46×10^{3}	0.943	−3.00	0.143	-5.86×10^{-2}	-2.70×10^{-2}	3.28×10^{-2}	2.17	4.13
6	1.42×10^{6}	1.22×10^{5}	1.83×10^{4}	-1.39×10^{3}	31.1	−1.26	−7.30×10^−2	9.37×10^{-2}	−0.145	−18.7	−40.5
7	8.57×10^{7}	3.21×10^{6}	-5.02×10^{3}	-2.92×10^{4}	3.46×10^{2}	4.55	2.09	−0.337	0.799	2.29×10^{2}	5.64×10^{2}
8	6.51×10^{9}	5.64×10^{7}	-2.20×10^{7}	-5.32×10^{4}	-5.25×10^{3}	55.2	−20.4	2.40	−13.7	-3.77×10^{3}	-1.06×10^{4}
9	5.93×10^{11}	-4.12×10^{9}	-1.78×10^{9}	2.93×10^{7}	-1.20×10^{5}	-1.62×10^{3}	-4.35×10^{2}	-3.84×10^{2}	2.73×10^{2}	8.05×10^{4}	2.57×10^{5}
10	6.13×10^{13}	-8.88×10^{11}	-1.01×10^{11}	1.50×10^{9}	1.43×10^{6}	0	-6.36×10^{4}	-2.95×10^{4}	-1.55×10^{4}	-2.16×10^{6}	-7.85×10^{6}
11	6.62×10^{15}	-1.16×10^{14}	-2.34×10^{12}	-5.74×10^{9}	1.98×10^{8}	-2.28×10^{7}	-9.16×10^{6}	-3.14×10^{5}	2.23×10^{6}	7.13×10^{7}	2.94×10^{8}
12	5.97×10^{17}	-1.17×10^{16}	4.59×10^{14}	-7.60×10^{12}	3.00×10^{11}	4.74×10^{9}	7.82×10^{8}	4.83×10^{8}	-4.13×10^{8}	-2.81×10^{9}	-1.33×10^{10}

We can perform the sum over V_{2n} in (5.3) by making use of the generating function for the vertices in (1.4):

$$\ln Z=\ln\left[\exp\left[\frac{G}{2}\frac{d^2}{dx^2}\right]\frac{F(x)}{F(0)}\right]_{x=0}. \tag{5.4}$$

By employing this generating function we take into account the delicate cancellations between graphs that occur in this model theory because of the variations in the signs of the vertices V_{2n}.

Using the expansion in (1.5) for $F(x)$ and expanding the exponential operator in (5.4) gives

$$\ln Z=\ln\left[1+\sum_{n=1}^{\infty}\frac{G^n}{2^n n!}\frac{\Gamma((2n+1)/\alpha)}{\Gamma(1/\alpha)}\right]. \tag{5.5}$$

Since we are in Region 2, $1\le\alpha<2$, the nth term of the sum in (4.5) grows rapidly with increasing n. In particular, the factor controlling the asymptotic behavior is

$$\frac{\Gamma((2n+1)/\alpha)}{n!}\approx n^{n(2/\alpha-1)}. \tag{5.6}$$

Thus, we can use the argument given at the beginning of Sec. II leading to (2.1). Therefore, as $n\to\infty$ an asymptotic approximation to the term containing G^n in (5.5) is

$$\frac{G^n}{2^n n!}\frac{\Gamma((2n+1)/\alpha)}{\Gamma(1/\alpha)}. \tag{5.7}$$

As discussed in Sec. I we obtain the perturbation coefficients C_n by including an extra factor of $2n$ [see the paragraph following (1.7)]:

$$C_n\approx\frac{2nG^n}{2^n n!}\frac{\Gamma((2n+1)/\alpha)}{\Gamma(1/\alpha)}. \tag{5.8}$$

This is the result for C_n obtained by making the drastic approximation that the lattice sum for each n-line graph may be replaced by its average value and that the average value has the form G^n. Note that this calculation gives a result for the sum over *all* n-line graphs which is dramatically smaller than the size of the dominant graphs discussed in Sec. IV which typically grow like $n!$. This is the simplest and cleanest demonstration we know which shows the large degree of cancellation that occurs in a theory whose graphs do not add in phase.

To complete this calculation we need a value for G. We obtain G empirically by determining the average size of a lattice sum for an n-line graph. Noting that the exact lattice sum for a graph is independent of α we define the average graph size G_n as follows: let $S_{i,n}$ be the symmetry number associated with the ith n-line graph. Let $I_{i,n}$ be the exact value of the lattice sum associated with that graph. Then G_n is the weighted average

$$G_n=\frac{\sum_i I_{i,n}S_{i,n}}{\sum_i S_{i,n}}, \tag{5.9}$$

where the sums are performed over all graphs having n-lines.

The denominator in (5.9) can be calculated analytically (see Appendices A and B). We have evaluated the numerator numerically for $n=1,2,3,\ldots,12$. The results for G_n are given in Table VII. Assuming that G_n has the

TABLE VII. The average graph size G_n determined from (5.8). For large n, G_n behaves very roughly like G^n where G is a constant lying between -2 and -2.5.

n	G_n	$\lvert G_n \rvert^{1/n}$
1	-2	2.0
2	5.333 33	2.309 39
3	-14.8571	2.458 36
4	41.1245	2.532 36
5	-112.502	2.571 77
6	303.308	2.592 07
7	-805.831	2.601 22
8	2110.61	2.603 46
9	-5453.08	2.601 25
10	13 906.88	2.596 11
11	$-35\,031.77$	2.589 01
12	87 221.20	2.580 59

form G^n, we obtain from Table VII a very rough estimate that G lies in the range $-2.5 < G < -2$.

To demonstrate that this graph-averaging technique gives a good description of the large-n behavior of C_n we compute the ratio

$$\lvert C_n \rvert \Big/ \left[\frac{2n\Gamma((2n+1)/\alpha)}{2^n n!\Gamma(1/\alpha)} \right], \tag{5.10}$$

and take the nth root of the result. We find (see Table VIII) that for the values $\alpha = 1$, 1.25, 1.5, and 1.75 these results are quite close to those in the third column of Table VII. These values give an estimate of the average graph size; the estimate for G obtained from Table VII and those given in Table VIII are independent of each other. The close agreement is an indication that the concept of an average graph size, independent of α, is meaningful even at these small values of n. We believe from a numerical analysis of the results in Table VII that $G = -2$.[8]

As α gets closer to two we find (not surprisingly) that the numbers are not in such good agreement. This is because as $\alpha \to 2$ the series in (5.5) becomes less divergent and thus the argument used in arriving at (5.8) becomes weaker in the sense that the leading term in the expansion of the logarithm in (5.5) is less dominant. Indeed, one can evaluate (5.5) numerically to determine the exact value of the approximation to C_n that it incorporates and verify that the approximation (5.8) is considerably more accurate at $\alpha = 1$ than at $\alpha = 2$.

To close this section we compare (see Table IX) the exact perturbation-series coefficients C_n to the approximate values for C_n obtained by the summation-of-dominant-graphs method of Sec. IV [see (4.12)] and by the graph-averaging method of this section. In the graph-averaging results we use (5.8) with the exact average graph sizes G_n given in the second column of Table VII instead of the estimates for G^n obtained by the method of Table VIII.

Note that the dominant-graph approximation gives numbers that are too small. Apparently, cancellations between dominant graphs reduce their net contribution to a size comparable to or less than that of individual graphs that were neglected in this approximation.

On the other hand, it is remarkable that an approximation as simple as graph averaging manages to give such an accurate result; statistical analysis of graphs is very difficult when they do not add in phase.

TABLE VIII. Values of

$$\{ \lvert C_n \rvert 2^n n!\Gamma(1/\alpha)/2n\Gamma((2n+1)/\alpha) \}^{1/n}$$

for $\alpha = 1, \frac{5}{4}, \frac{3}{2}, \frac{7}{4}$. These values give an estimate of the average graph size, as discussed in the paragraph containing (5.9). Note that these values are in approximate agreement with the independent estimate of the average graph size in the third column of Table VII. Notice also that the entries in this table increase to a maximum, which depends weakly on α, and then decrease.

n \ α	1	5/4	3/2	7/4
1	2.0000	2.0000	2.0000	2.0000
2	2.0000	2.0000	2.0000	2.0000
3	2.0987	2.1371	2.1659	2.1866
4	2.1506	2.2322	2.2969	2.3445
5	2.1711	2.2921	2.3931	2.4691
6	2.1746	2.3285	2.4639	2.5680
7	2.1691	2.3498	2.5167	2.6477
8	2.1595	2.3611	2.5564	2.7128
9	2.1462	2.3657	2.5867	2.7669
10	2.1367	2.3659	2.6098	2.8122
11	2.1256	2.3632	2.6275	2.8507
12	2.1154	2.3586	2.6410	2.8836

VI. REGION 2: $1 \leq \alpha < 2$. LATTICE INSTANTON CALCULATION

In this section we apply a Lipatov approach[1] to the problem of determining the large-order behavior of the perturbation coefficients C_n. In this approach one writes a functional integral representation for the nth perturbation-theory coefficient and applies a saddle-point method to find the asymptotic behavior for large n. The saddle point is a point in function space called an instanton that satisfies the field equations and gives a finite contribution to the action when the method is successful.

In contrast to the usual continuum applications of the instanton method, in the lattice strong-coupling theory the classical field equations that determine the instanton are finite-difference equations on the lattice. As a result we must deal with two different limits: the limit $n \to \infty$ and the limit in which the number of lattice points $\to \infty$. Although we have succeeded in extracting the controlling factor in the asymptotic behavior of C_n we are unable to complete the instanton analysis and determine the full asymptotic behavior of C_n. The difficulty is related both to the ambiguity in the order of the two limits and to the problem of finding an instanton solution to the finite-difference field equations that yields finite action.

We begin with the Euclidean functional integral representation for the ground-state energy $E_0(\alpha)$ for the Hamiltonian H (1.1):

$$e^{-VE_0(\alpha)} = \int D\Psi \exp\left[-\int (\tfrac{1}{2}\Psi^2 + g \lvert \Psi \rvert^{\alpha}) dt \right], \tag{6.1}$$

where V is the volume of space. On the lattice $V = Na$,

TABLE IX. Comparison of the exact perturbation series coefficients C_n, the approximate values calculated by the method of dominant graphs in Sec. IV, and the graph-averaging method of Sec. V. (a) $\alpha=1$, (b) $\alpha=\frac{5}{4}$, (c) $\alpha=\frac{3}{2}$, (d) $\alpha=\frac{7}{4}$.

n	Exact C_n	Dominant graphs	Graph averaging
		(a) $\alpha=1$	
1	-4.0	-4.0	-4.0
2	48.0	72.0	64.0
3	-8.32×10^{2}	-6.7×10^{2}	-1.3×10^{3}
4	1.8×10^{4}	1.2×10^{4}	3.5×10^{4}
5	-4.6×10^{5}	-2.3×10^{5}	-1.1×10^{6}
6	1.3×10^{7}	5.5×10^{6}	3.8×10^{7}
7	-4.3×10^{8}	-1.5×10^{8}	-1.5×10^{9}
8	1.5×10^{10}	4.9×10^{9}	6.8×10^{10}
9	-6.0×10^{11}	-1.7×10^{11}	-3.4×10^{12}
10	2.6×10^{13}	7.0×10^{12}	1.8×10^{14}
11	-1.2×10^{15}	-3.1×10^{14}	-1.1×10^{16}
12	6.1×10^{16}	1.5×10^{16}	6.6×10^{17}
		(b) $\alpha=\frac{5}{4}$	
1	-2.1	-2.1	2.1
2	10.0	17.0	14.0
3	-65.0	-40.0	-98.0
4	4.7×10^{2}	1.9×10^{2}	7.7×10^{2}
5	-3.7×10^{3}	-6.8×10^{3}	-6.6×10^{3}
6	3.2×10^{4}	2.8×10^{3}	6.1×10^{4}
7	-2.9×10^{5}	-8.8×10^{3}	-6.0×10^{5}
8	2.8×10^{6}	1.4×10^{4}	6.2×10^{6}
9	-2.9×10^{7}	1.4×10^{5}	-6.8×10^{7}
10	3.0×10^{8}	-2.0×10^{6}	7.7×10^{8}
11	-3.3×10^{9}	1.5×10^{7}	-9.1×10^{9}
12	3.8×10^{10}	-6.6×10^{7}	1.1×10^{11}
		(c) $\alpha=\frac{3}{2}$	
1	-1.5	-1.5	-1.5
2	4.1	7.4	5.5
3	-14.0	-5.7	-20.0
4	51.0	11.0	76.0
5	-2.0×10^{2}	-2.9	-2.9×10^{2}
6	8.6×10^{2}	-9.3	1.2×10^{3}
7	-3.7×10^{3}	38.0	-4.7×10^{3}
8	1.7×10^{4}	-12.0	1.9×10^{4}
9	-7.7×10^{4}	-2.3×10^{2}	-8.1×10^{5}
10	3.6×10^{5}	7.6×10^{2}	3.4×10^{5}
11	-1.7×10^{6}	-4.1×10^{2}	-1.5×10^{6}
12	8.6×10^{6}	2.8×10^{4}	6.5×10^{6}
		(d) $\alpha=\frac{7}{4}$	
1	-1.2	-1.2	-1.2
2	2.3	4.3	3.0
3	-5.0	-1.0	-7.1
4	12.0	0.93	16.0
5	-30.0	0.91	-37.0
6	78.0	-0.46	83.0
7	-2.0×10^{2}	-0.95	-1.8×10^{2}
8	5.6×10^{2}	1.1	4.0×10^{2}
9	-1.5×10^{3}	1.7	-8.8×10^{2}
10	4.3×10^{3}	-4.4	1.9×10^{3}
11	-1.2×10^{4}	31.0	-4.2×10^{3}
12	3.4×10^{4}	-8.6×10^{2}	9.0×10^{3}

where a is the lattice spacing and N is the number of lattice points. Therefore, the lattice version of (6.1) is

$$e^{-NaE_0(\alpha)}=\int\prod_{i=0}^{N}\frac{d\Psi_i}{\sqrt{2\pi a}}e^{-L}, \tag{6.2}$$

where

$$L=a\sum_{i=0}^{N-1}\frac{1}{2}\left[\frac{\Psi_{i+1}-\Psi_i}{a}\right]^2+ga\sum_{i=0}^{N}|\Psi_i|^{\alpha}. \tag{6.3}$$

Solve for $E_0(\alpha)$ by calculating the logarithmic derivative of (6.2) with respect to the coupling strength g:

$$\frac{Na\,dE_0(\alpha)}{dg}=\frac{a\int\prod_{i=0}^{N}(d\Psi_i/\sqrt{2\pi a})e^{-L}\sum_{j=0}^{N}|\Psi_i|^{\alpha}}{\int\prod_{i=0}^{N}(d\Psi_i/\sqrt{2\pi a})e^{-L}}. \tag{6.4}$$

Each term in the numerator sum contributes equally, because of translation invariance. Using this fact and (1.2) we obtain

$$\epsilon(\alpha)=\frac{\alpha+2}{2}\frac{g^{\alpha/(\alpha+2)}\int\prod_{i=0}^{N}(d\Psi_i/\sqrt{2\pi a})e^{-L}|\Psi_j|^{\alpha}}{\int\prod_{i=0}^{N}(d\Psi_i/\sqrt{2\pi a})e^{-L}}, \tag{6.5}$$

where j is any integer between 0 and N. We now introduce the dimensionless lattice parameter $x=g^{-2/\alpha}a^{-(2+\alpha)/\alpha}$ and the dimensionless lattice field $\varphi_i=(ax)^{-1/2}\psi_i$. Thus,

$$L=\tfrac{1}{2}x\sum_{i=0}^{N-1}(\varphi_{i+1}-\varphi_i)^2-\sum_{i=0}^{N}|\varphi_i|^{\alpha} \tag{6.6}$$

and

$$\epsilon(d)=\frac{\alpha+2}{2}x^{\alpha/(\alpha+2)}\frac{\int\prod_{i=1}^{N}d\varphi_i e^{-L}|\varphi_j|^{\alpha}}{\int\prod_{i=0}^{N}d\varphi_i e^{-L}}, \tag{6.7}$$

where the continuum limit $x\to\infty$ is understood. Comparing (6.7) with (1.3) one finds

$$C_n=\text{coefficient of } x^n \text{ in}\left[\frac{\alpha\int\prod_{i=0}^{N}d\varphi_i e^{-L}|\varphi_j|^{\alpha}}{\int\prod_{i=0}^{N}d\varphi_i e^{-L}}\right]. \tag{6.8}$$

It has already been argued that the series $\sum C_n x^n$ is divergent when $0<\alpha<2$. If $\sum C_n x^n=\sum a_n x^n/\sum b_n x^n$, where the series on the right-hand side represents the numerator and denominator of (6.8) and are divergent, it follows that $C_n\sim(a_n-C_0b_n)/b_0$ as $n\to\infty$. A scaling argument suggests that b_n is negligible compared to a_n as $n\to\infty$.

Let $\varphi_i=n^{1/\alpha}\sigma_i$. Then

$$L=\tfrac{1}{2}xn^{2/\alpha}\sum_{i=0}^{N-1}(\sigma_{i+1}-\sigma_i)^2+n\sum_{i=0}^{N}|\sigma_i|^{\alpha} \tag{6.9}$$

and

$$C_n=\text{coefficient of } x^n \text{ in}\times\left[\frac{n\alpha\int\prod_{i=0}^{N}d\sigma_i e^{-L}|\sigma_j|^{\alpha}}{\int\prod_{i=0}^{N}d\sigma_i e^{-L}}\right]. \tag{6.10}$$

Thus, b_n is smaller than a_n by a factor of n and we have

$$C_n\sim a_n/b_0,\quad n\to\infty. \tag{6.11}$$

It is easy to evaluate the expression

$$b_0=\left[\int_{-\infty}^{\infty}d\varphi\, e^{-|\varphi|^{\alpha}}\right]^N \tag{6.12}$$

by the substitution $t=\varphi^{\alpha}$. The result is

$$b_0=\left[2\Gamma\left(1+\frac{1}{\alpha}\right)\right]^N. \tag{6.13}$$

To compute a_n by the Lipatov technique, express a_n as a contour integral over the numerator of (6.10):

$$a_n=n^{N/\alpha}\frac{n\alpha}{2\pi i}\oint\frac{dx}{x}e^{-n\ln x}\prod_{i=0}^{N}d\sigma_i e^{-L}|\sigma_j|^{\alpha}, \tag{6.14}$$

where L is given by (6.9). Next, make the substitution $x=n^{1-2/\alpha}y$ and use (6.13) to obtain

$$C_n\sim\frac{(-1)^n n^{N/\alpha}n\alpha n^{(2/\alpha-1)n}}{2^N\Gamma(1+1/\alpha)^N}\frac{1}{2\pi i}\times\oint\frac{dy}{y}\int\prod_{i=0}^{N}d\sigma_i|\sigma_j|^{\alpha}e^{-nL}, \tag{6.15}$$

where

$$L=\ln(-y)+\tfrac{1}{2}y\sum_{i=0}^{N-1}(\sigma_{i+1}-\sigma_i)^2+\sum_{i=0}^{N}|\sigma_i|^{\alpha}. \tag{6.16}$$

Notice that the integral in (6.15) is now in standard Laplace form, $\int e^{nf(\psi)}D\psi$; this was the goal of the scaling manipulations. In a conventional analysis one would now proceed as follows: locate the maximum of f and argue that the integral is dominated by this contribution, with Gaussian corrections. The general result of such a treatment is typically an asymptotic behavior for the integral of the form $e^{nf(\psi_{\max})}\times(\text{algebraic terms}\sim n^c)$, $n\to\infty$.

There are, however, several problems with (6.15). First, (6.15) contains an explicit factor $[n^{1/\alpha}/2\Gamma(1+1/\alpha)]^N$ where N is the number of lattice points and n is the order of perturbation theory (the number of lines). Implicit in our lattice analysis is the idea that N is large, but fixed, and that the perturbation coefficients do not depend on N. The limit $n\to\infty$, for a quality that depends explicitly on N, is not well defined.

Moreover, the detailed application of the Laplace argu-

ment requires that one locate the maximum of L in (6.16) by differentiating with respect to y and the σ_i. Because L involves $|\sigma_i|^\alpha$, the action is not continuously differentiable. If we nevertheless solve the resulting difference equations the action is not finite at the location of the instanton solution.

Finally, the integral in (6.15) involves both N and n. If $n \to \infty$ for fixed N, the number of lines becomes large with respect to the number of available lattice points, which implies that most of the graphs are neglected.

Nevertheless, we emphasize that (6.15) has the form

$$C_n \sim n^{(2/\alpha-1)n} \times (\text{algebraic factors}) \times (\text{Laplace integral}) .$$

Because the Laplace integral cannot give an n dependence stronger than exponential, there is good reason to believe that the controlling behavior of C_n has been successfully identified as

$$C_n \sim n^{(2/\alpha-1)n}, \quad n \to \infty . \tag{6.17}$$

Note that this agrees with the controlling factor of the result (5.8) obtained by graph averaging.

VII. REGION 3. THE INTRACTABLE RANGE $\alpha > 2$

Of the three methods used in Secs. IV–VI to analyze the large-n behavior of C_n the simplest and most effective is the average graph approach of Sec. V. It is clear from (5.8) that this approximation must fail in Region 3 because (5.8) predicts that C_n alternates in sign. However, we know (see Ref. 4) that the sign pattern of C_n is irregular.

A tempting explanation of this failure is the following. To obtain (5.8) we asymptotically expanded the logarithm in (5.5). The expansion used is valid in Region 2 because the series in (5.5) is divergent for $\alpha < 2$. However, when $\alpha > 2$ the asymptotic expansion is invalid and (5.8) cannot represent the behavior of C_n for large n. A direct remedy for this problem is to evaluate the Taylor series of (5.5) exactly (using MACSYMA). Unfortunately, while the resulting numerical values for C_n now have an irregular sign pattern, it is the wrong sign pattern. Moreover, the prediction for $|C_n|$ is wrong by many orders of magnitude. The other approaches in Secs. IV and VI also fail when $\alpha > 2$.

Apparently the reason for this failure is that the cancellation between graphs (which produces a convergent lattice perturbation series for $\alpha > 2$) is very subtle. No graph-averaging technique is delicate enough to accurately embody these cancellations and no simple topological class of graphs seems to dominate in the presence of such cancellations. The cancellations appear to occur on a graph-by-graph basis and we know of no asymptotic approximation that can successfully predict the behavior of C_n for large n.

This difficulty appears to be generic to the class of field theories having convergent perturbation expansions. We know of no example of an asymptotic analysis which correctly predicts a nonzero radius of convergence of the perturbation expansion of a field theory. We therefore believe that continued study of this very simple model field theory for the region $\alpha > 2$ is worthwhile because a successful technique might well generalize to the case of more complicated realistic theories.

ACKNOWLEDGMENTS

We are indebted to the MIT Laboratory for Computer Science for allowing us the use of MACSYMA for algebraic manipulation. This work was supported by the U.S. Department of Energy.

APPENDIX A: ASYMPTOTIC ESTIMATES OF THE NUMBER OF GRAPHS

We define the *number of graphs* A_n of order n as follows: Assign to each graph its appropriate symmetry number and sum over all graphs with n lines. In this appendix we study the asymptotic growth of the number of lattice strong-coupling graphs for large order n, where n is the number of lines. We then verify these estimates by comparing them with exact computer calculations of the number of graphs for small and intermediate values of n. The result gives an asymptotic estimate, for large n, of the denominator in (5.9).

We compute A_n by means of a generating function, $Z(x,\epsilon)$:

$$Z(x,\epsilon) \equiv \exp\left[\tfrac{1}{2}\epsilon \frac{d^2}{dx^2}\right] \exp\left[\sum_{k=0}^{\infty} \frac{x^{2k}}{(2k)!}\right] . \tag{A1}$$

The operator $\exp(\frac{1}{2}\epsilon d^2/dx^2)$ is a line-insertion operator, so each line will be associated with one power of ϵ. Therefore, if Z is expanded as a series in powers of ϵ, the coefficient of ϵ^n is the number of graphs having n lines. The factor $\frac{1}{2}$ occurs in this operator because the lines in this theory are not directional. The factor

$$\exp\left[\sum_{k=1}^{\infty} \frac{x^{2k}}{(2k)!}\right]$$

inserts all vertices with an even number of lines and gives each vertex unit weight. The factor $1/(2k)!$ is necessary to avoid overcounting because all the lines at a given vertex are identical.

The variable x plays the role of the external current in this model quantum field theory in zero-dimensional space-time. Therefore, if Z is expanded as a series in powers of x, the coefficient of x^l is the number of graphs having l external legs. In this paper we consider only vacuum, or bubble, graphs (graphs having no external legs). Thus to obtain A_n we evaluate Z at $x=0$:

$$Z(0,\epsilon) = 1 + \sum_{n=1}^{\infty} A_n \epsilon^n . \tag{A2}$$

A_n includes all n-line graphs, disconnected as well as connected. To obtain B_n, the number of connected graphs having n lines, we construct $W \equiv \ln Z$, which is the generating function for the connected graphs:

$$W(\epsilon) = \sum_{n=1}^{\infty} B_n \epsilon^n . \tag{A3}$$

We shall show that A_n grows sufficiently rapidly with n so that the argument leading to (2.3) applies and therefore

$$A_n \sim B_n \quad (n \to \infty) . \tag{A4}$$

To find the asymptotic behavior of A_n as $n \to \infty$ we begin by writing

$$Z(x,\epsilon) = \exp\left[\tfrac{1}{2}\epsilon \frac{d^2}{dx^2}\right] e^{\cosh x - 1} .$$

Thus, from (A2),

$$A_n = \frac{1}{e n! 2^n} \frac{d^{2n}}{dx^{2n}} e^{\cosh x}\bigg|_{x=0} . \tag{A5}$$

Using the generating function[9] for the associated Bessel functions, we have the following identity:

$$e^{t\cosh x} = \sum_{k=-\infty}^{\infty} I_k(t) e^{kx} . \tag{A6}$$

Using this formula we can express A_n in (A5) as the infinite sum

$$A_n = \frac{2}{e n! 2^n} \sum_{k=1}^{\infty} I_k(1) k^{2n} . \tag{A7}$$

The result in (A7) is exact. To obtain the asymptotic behavior of A_n for n large, we approximate the sum in (A7) using a discrete Laplace's method. That is, we identify the value of k for which the summand in (A7) is maximum. Then we approximate the nearby terms in the sum by a Gaussian. The Gaussian sum when evaluated by replacing it by a Riemann integral gives the leading approximation to A_n for large n.

As $n \to \infty$ it is clear that the sum in (A7) is dominated by large values of k. Thus, it is correct to approximate $I_k(1)$ by its asymptotic behavior for large k (Ref. 10):

$$I_k(1) \sim \frac{2^k}{k!} \quad (k \to \infty) . \tag{A8}$$

This gives the following approximation to (A7):

$$A_n \sim \frac{\sqrt{2}}{e\sqrt{\pi} n! 2^n} \sum_{k=1}^{\infty} \frac{1}{\sqrt{k}} e^{\varphi(k)} \quad (n \to \infty) , \tag{A9}$$

$$\varphi(k) = 2n \ln k + k - k \ln(2k) , \tag{A10}$$

where we have used Stirling's formula to approximate $k!$ in (A8).

$\varphi(k)$ attains its maximum at $k = k_0$, the solution to

$$k_0 \ln(2k_0) = 2n . \tag{A11}$$

Noting that $\varphi''(k) = -2n/k^2 - 1/k$, a Gaussian approximation to the summand in (A9) is

$$A_n \sim \frac{2}{\pi k_0} \frac{1}{e n! 2^n} \exp[2n \ln k_0 + k_0 - k_0 \ln(2k_0)] \times \sum_{k=-\infty}^{\infty} \exp\left[-\frac{1}{2}\left[\frac{1}{k_0} + \frac{2n}{k_0^2}\right](k-k_0)^2\right] . \tag{A12}$$

Finally, we use a Reimann integral to approximate the sum

$$\sum_{k=-\infty}^{\infty} e^{-k^2\epsilon^2} \sim \frac{1}{\epsilon} \int_{-\infty}^{\infty} e^{-x^2} dx = \frac{\sqrt{\pi}}{\epsilon} \quad (\epsilon \to \infty) .$$

Thus,

$$A_n \sim \frac{2\exp(-2n + k_0 + 2n \ln k_0)}{e n! 2^n [1 + \ln(2k_0)]^{1/2}} \quad (n \to \infty) . \tag{A13}$$

Note that A_n grows with n slightly less rapidly than $n!$; very roughly, $A_n \approx n!/[\ln(2n)/\sqrt{2}]^{2n}$. This growth, however, is sufficiently rapid to allow us to invoke the argument given in Sec. II, and to conclude that $A_n \sim B_n$.

We used MACSYMA to calculate the exact value of A_n and B_n for $1 \le n \le 30$ from (A5) and (A3). The first six of these are $A_1 = \frac{1}{2}$, $A_2 = \frac{1}{2}$, $A_3 = \frac{31}{48}$, $A_4 = \frac{379}{384}$, $A_5 = \frac{1639}{960}$, $A_6 = \frac{150\,349}{46\,080}$, and $B_1 = \frac{1}{2}$, $B_2 = \frac{3}{8}$, $B_3 = \frac{7}{16}$, $B_4 = \frac{83}{128}$, $B_5 = \frac{287}{256}$, $B_6 = \frac{33\,371}{15\,360}$. In Table X we compare the asymptotic formula (A13) for the number of graphs with the exact numerical values of A_n and B_n for $n = 20, 25, 30$.

APPENDIX B: STATISTICAL ANALYSIS OF GRAPHS

In this appendix we carry out a statistical analysis whose purpose is to characterize topologically the class of graphs that dominates the asymptotic estimate given in (A13) for the total number of graphs A_n (connected or disconnected).

Graphs containing n lines can have from one to n vertices. This divides the set of all n-line graphs into n topologically distinct classes labeled by an integer j, $1 \le j \le n$, where class j has j vertices. We define $A_{n,j}$ to be the number of graphs having n lines and j vertices so

$$\sum_{j=1}^{n} A_{n,j} = A_n . \tag{B1}$$

TABLE X. Comparison between the exact total number of graphs A_n, the exact total number of connected graphs B_n, and the asymptotic estimate given by (A13).

n	20	25	30
k_0	12.444	14.768	17.011
Exact A_n	$9.627\,15 \times 10^6$	$9.978\,01 \times 10^9$	$1.831\,12 \times 10^{13}$
A_n from (A13)	9.5215×10^6	9.8836×10^9	1.8158×10^{13}
% relative error between (A13) and A_n	−1.10	−0.95	−0.83
Exact B_n	$8.029\,83 \times 10^6$	$8.578\,09 \times 10^9$	$1.605\,92 \times 10^{13}$
% relative error between (A13) and B_n	18.6	15.2	13.1

We further subdivide the jth class according to the specific types of vertices present. That is, if $2a_i$ is the number of lines at the ith vertex then

$$\sum_{i=1}^{j} a_i = n \ . \tag{B2}$$

Thus, the set $\{a_1,a_2,\ldots,a_j\}$ is a partition of n and the number of subdivisions of the jth class is equal to the number of partitions of the integer n.

The analysis of this appendix is a statistical analysis of graphs having many lines. First, we fix the number of vertices j and analytically determine the distribution of vertices $\{a_1,a_2,\ldots,a_j\}$ that dominates the sum over partitions contributing to $A_{n,j}$. Then we determine the value of j for which $A_{n,j}$ dominates the sum in (B1). We verify our analytic results by comparing them with exact numerical values of $A_{n,j}$.

The total number of diagrams belonging to the partition $\{a_1,a_2,\ldots,a_j\}$ is exactly

$$(2n-1)!!\Big/\left[j!\prod_{k=1}^{j}(2a_k)!\right] \ . \tag{B3}$$

We derive this result as follows: Consider a set of j vertices, the kth vertex having $2a_k$ free lines emerging from it. To construct the graphs in this partition pick an arbitrary free line and join it to any other free line. There are

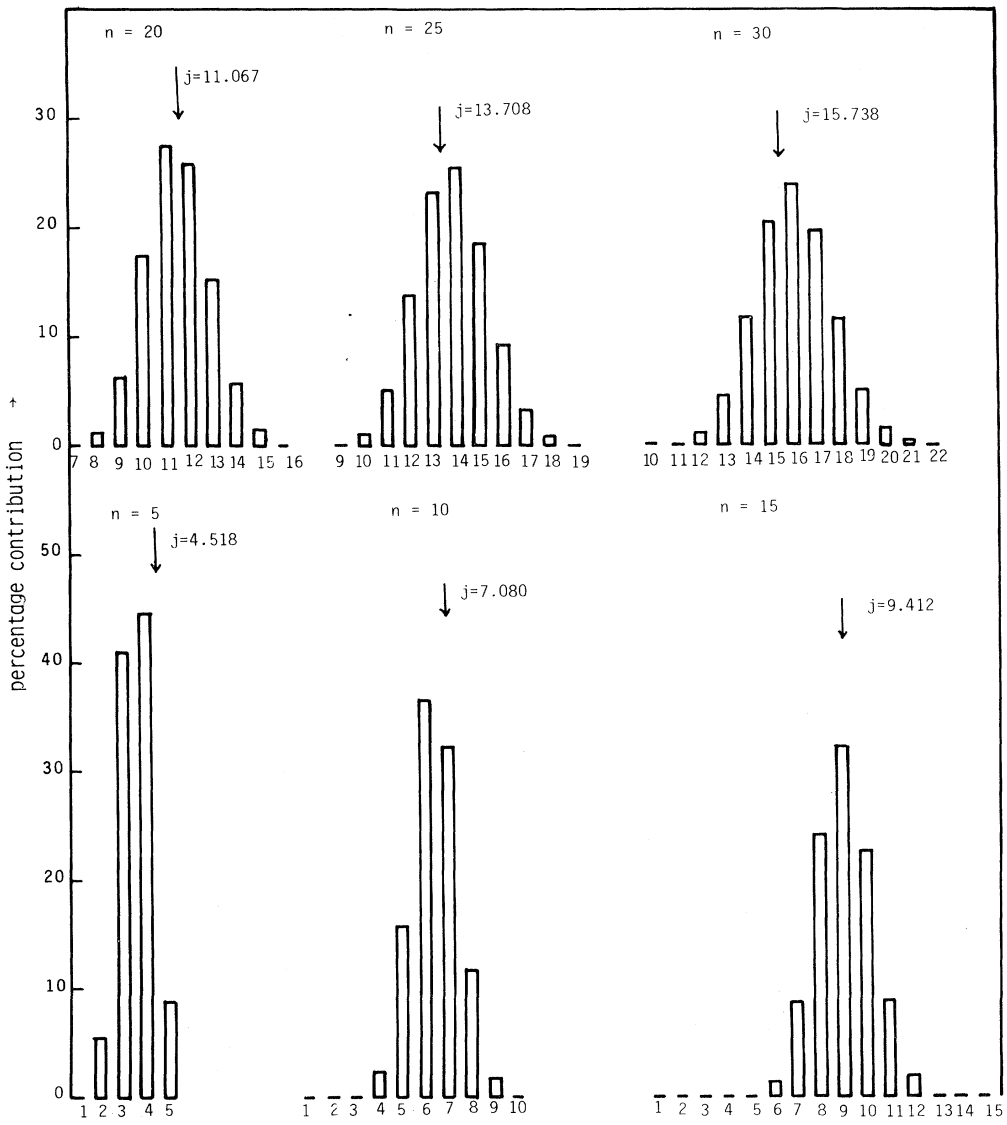

FIG. 7. Histograms displaying the results of a computer calculation of the number of n-line graphs with j vertices, as a percentage of the total number of n-line graphs, for $n=5$, 10, 15, 20, 25, and 30. The values of j in the calculation range from one to n but values of j for which the ordinate is $<10^{-3}$ are not shown. The arrow on each histogram marks the asymptotic prediction in (B14) for the dominant value of j. Note that the distribution of graph numbers are sharply peaked about a central value that agrees very closely with (B14).

$2n-1$ choices. Next pick one of the remaining free lines and join it to any of the $(2n-3)$ other free lines. Repeat this process until no free lines remain. The number of graphs constructed using this procedure is $(2n-1)!!$. However, this enormously overcounts the number of *distinct* graphs in this partition. We must reduce this total by the number of ways $j!$ of relabeling the vertices. Furthermore, the lines emerging from the kth vertex are identical so we must divide by $(2a_k)!$ for the kth vertex.

Summing over all partitions $\{a_1,a_2,\ldots,a_j\}$ having j vertices subject to the constraint in (B2) we obtain the total number of graphs with n lines and j vertices:

$$A_{n,j}=\frac{(2n-1)!!}{j!}\sum_{\text{all } a_k}\frac{1}{\prod_{i=0}^{j}(2a_k)!}\,. \tag{B4}$$

This result is exact.

In order to obtain an asymptotic evaluation of (B4) we want to identify the partition that dominates this sum. We begin by using Stirling's formula to approximate the factorials in (B4), assuming that each of the a_k is large (our final result is consistent with this assumption):

$$A_{n,j}\sim\frac{(2n-1)!!}{j!}\frac{e^{2n}}{(2\pi)^{j/2}}\times\sum_{\text{all } a_k}\exp\left[-\sum_{k=1}^{j}(2a_k+\tfrac{1}{2})\ln(2a_k)\right]\quad(j,n\to\infty)\,, \tag{B5}$$

subject to the constraint in (B2).

One way to achieve an asymptotic evaluation of (B5) is to make a continuum approximation to the sum over the a_k. Introduce the continuous variable

$$t=k/j,\quad 0<t\leq 1 \tag{B6}$$

and replace the discrete function a_i by a continuous function $a(t)$:

$$a_k=\frac{n}{j}a(t)\,. \tag{B7}$$

The constraint in (B2) becomes

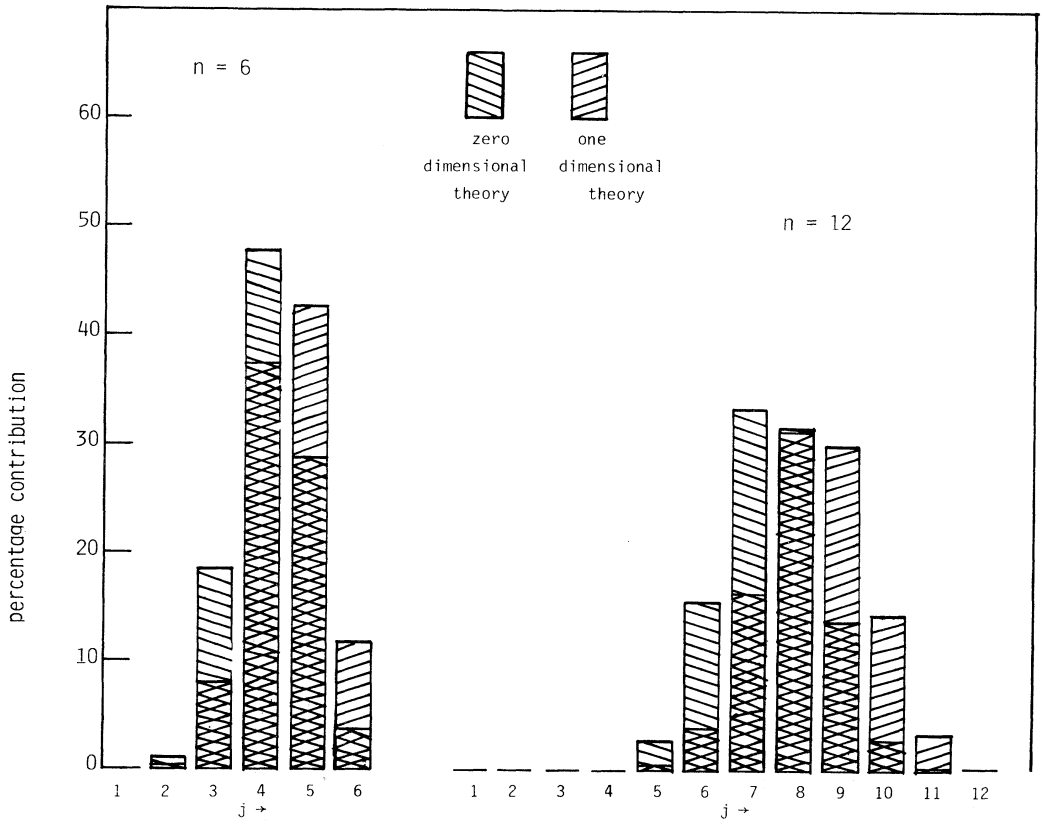

FIG. 8. Comparison of the relative sizes of $A_{n,j}$ for the zero-dimensional pure graph-counting case considered in Appendix B (in which all lattice sums have the value one) and the one-dimensional case considered in the body of the paper (in which lattice sums are evaluated as explained in Sec. I). The histograms display the number of n-line graphs with j vertices as a percentage of the total number of n-line graphs. Observe that the location of the maximum value of $A_{n,j}$ and the widths of the distributions are almost independent of the dimension.

$$\int_0^1 dt\, a(t)=1 \ . \tag{B8}$$

Note that the normalization factor n/j in (B7) was chosen so that $a(t)=O(1)$ and (B8) contains no large or small parameters.

In terms of the new variables, the sum in (B5) becomes a functional integral:

$$A_{n,j}\sim\frac{(2n-1)!!}{j!}\exp\left[2n-(2n+\tfrac{1}{2})\ln\left[\frac{2n}{j}\right]\right]\int Da\exp\left\{-\int_0^1 dt[\tfrac{1}{2}j+2na(t)]\ln a(t)\right\}\quad(j,n\to\infty)\ , \tag{B9}$$

where Da stands for

$$\lim_{j\to\infty}\prod_{k=1}^{j}da_k\Big/\sqrt{2\pi}\ ,$$

and the constraint in (B8) is understood. We can apply Laplace's method to this functional integral. Let

$$L=-\int_0^1 dt[\tfrac{1}{2}j+2na(t)]\ln a(t)+\lambda\left[\int_0^1 dt a(t)-1\right], \tag{B10}$$

where λ is a Lagrange multiplier that ensures the constraint (B8).

We now vary L with respect to λ and $a(t)$ to establish the stationary point in $(\lambda-a)$ space, which dominates the integrand of (B9). Varying with respect to λ reproduces the constraint (B8):

$$\frac{\delta L}{\delta a(t)}=\lambda-\frac{1}{2}\frac{j}{a(t)}-2n-2n\ln a(t)=0\ . \tag{B11}$$

Because (B11) does not depend explicitly on t, it follows that $a(t)$ is a constant, and from (B8) we have

$$a(t)=1\ . \tag{B12}$$

With (B7) this establishes that the distribution of vertices $\{a_1,a_2,\ldots,a_j\}$ that dominates the sum over partitions contributing to $A_{n,j}$ is flat: $\{n/j,n/j,\ldots,n/j\}$ (j terms). That is, the dominant partition is that in which each of the j vertices is the same, with $2n/j$ lines at each vertex

We have shown that $a(t)=1$ is the saddle point that dominates (B9). Therefore, apart from Gaussian corrections,

$$A_{n,j}\sim\frac{(2n-1)!!\exp[2n-(2n+\frac{1}{2}j)\ln 2n/j]}{j!(2\pi)^{j/2}}\ . \tag{B13}$$

Now we are prepared to answer the question posed at the beginning of this appendix; to find the class of graphs that dominates the asymptotic estimate (A13) for the total number of graphs. The dominant value of j in (B13) is determined by $dA_{n,j}/dj=0$, which implies that

$$\frac{2n+\frac{1}{2}}{j}-\tfrac{1}{2}\ln j-\tfrac{1}{2}\ln 4\pi n+\tfrac{1}{2}=0\ . \tag{B14}$$

Numerical solutions to this equation are shown in Fig. 7.

To provide a check on the asymptotic analysis resulting in (B14) we calculate $A_{n,j}$ numerically using a procedure based on a generating function similar to that in (A1). Consider the generating function

$$Z(x,L,V)\equiv\exp\left[\tfrac{1}{2}L\frac{d^2}{dx^2}\right]\exp\left[V\sum_{n=1}^{\infty}\frac{x^{2n}}{(2n)!}\right]\ . \tag{B15}$$

In the Taylor expansion of (B15), the coefficient of L^nV^j is $A_{n,j}$. In Fig. 7 we show histograms of the relative numbers of nth-order graphs with j vertices (with the total number of graphs normalized to 100%). The dominant value of j calculated from (B14) is also shown. Note that the distributions are sharply peaked about values of j that agree well with the predictions of (B14) and that the agreement improves with increasing n.

Finally, we also calculated the distribution of $A_{n,j}$ versus j for the one-dimensional field theory described in Sec. I, using MACSYMA to evaluate the lattice sums. In Fig. 8 we compare histograms of the relative numbers of 6th- and 12th-order graphs with j vertices for this one-dimensional theory with the results for the zero-dimensional theory of (B15). The location of the maximum value of $A_{n,j}$ and the widths of the distributions are almost independent of the dimension. This shows that in a statistical analysis of graphs, the graph-counting considerations seem to be more important than the rules for computing lattice sums.

[1]For a good summary of this field see Int. J. Quant. Chem. 21 (1982). This issue reports the proceedings of the 1981 International Workshop on Perturbation Theory in Large Order. A complete collection of references is given therein.

[2]See, for example, M. L. Laursen, and M. A. Samuel, Phys. Lett. 91B, 249 (1980); Phys. Rev. D 23, 2478 (1981); J. Math. Phys. 22, 1114 (1981).

[3]For a study of asymptotic estimates in the many-fermion case, see G. A. Baker, Jr. and H. J. Pirner, Ann. Phys. (N.Y.) 148, 168 (1983).

[4]See C. M. Bender, L. R. Mead, and L. M. Simmons, Jr., Phys. Rev. D 24, 2674 (1981).

[5]C. M. Bender and S. A. Orszag, *Advanced Mathematical Methods for Scientists and Engineers* (McGraw-Hill, New York, 1978).

[6]See, for example, M. A. Evgrafov, *Asymptotic Estimates and Entire Functions* (Gordon and Breach, New York, 1961), p. 105.

[7]C. M. Bender and T. T. Wu, Phys. Rev. Lett. 37, 117 (1976).

[8]Strong evidence that $G=-2$ comes from the fact that the approximations in (4.12) and (5.8) when evaluated at $\alpha=1$ predict the same controlling factor. Substituting $\alpha=1$ in (4.12), one can easily perform the double summation over l and j. Using the value of V_{2n} in (1.11) one can also perform the sum over k in closed form. The result is $C_n \approx (-1)^n \frac{4}{9}(2n)!/(n-1)!$. The approximation in (5.8), evaluated for $\alpha=1$, gives $C_n \approx 2(G/2)^n(2n)!/(n-1)!$. These two results are consistent for $G=-2$.

[9]*Handbook of Mathematical Functions,* edited by M. Abramowitz and I. A. Stegun (U.S. GPO, Washington, D.C., 1964), (9.6.33).

[10]To derive the result in Eq. (A8) we use the Taylor-series expansion

$$I_\gamma(z)=\sum_{n=0}^{\infty}\frac{(\frac{1}{2}z)^{\gamma+2n}}{n!\Gamma(n+\gamma+1)}$$

and observe that as $\gamma\to\infty$ for fixed z the first term in the sum dominates. We warn the reader that the formula (8) in 7.13.2 of A. Erdelyi *et al.*, *Higher Transcendental Functions* (McGraw-Hill, New York, 1956), Volume II, p. 86 is incorrect. It is wrong by a factor $\sqrt{\pi}$.